NeuroImage 184 (2019) 25–35

Contents lists available at ScienceDirect

NeuroImage

journal homepage: www.elsevier.com/locate/neuroimage

Inhibitory and excitatory mechanisms in the human cingulate-cortex support reinforcement learning: A functional Proton Magnetic Resonance Spectroscopy study

Vered Bezalel [a,b], Rony Paz [a,*,1], Assaf Tal [b,*,1]

[a] Department of Neurobiology, Weizmann Institute of Science, Israel
[b] Department of Chemical and Biological Physics, Weizmann Institute of Science, Israel

ARTICLE INFO

Keywords:
Anterior cingulate cortex
fMRS
GABA
E/I-balance
Reinforcement learning

ABSTRACT

The dorsal anterior cingulate cortex (dACC) is crucial for motivation, reward- and error-guided decision-making, yet its excitatory and inhibitory mechanisms remain poorly explored in humans. In particular, the balance between excitation and inhibition (E/I), demonstrated to play a role in animal studies, is difficult to measure in behaving humans. Here, we used functional magnetic-resonance-spectroscopy (^{1}H-fMRS) to measure the brain's major inhibitory (GABA) and excitatory (Glutamate) neurotransmitters during reinforcement learning with three different conditions: high cognitive load (uncertainty); probabilistic discrimination learning; and a control null-condition. Participants learned to prefer the gain option in the discrimination phase and had no preference in the other conditions. We found increased GABA levels during the uncertainty condition, potentially reflecting recruitment of inhibitory systems during high cognitive load when trying to learn. Further, higher GABA levels during the null (baseline) condition correlated with improved discrimination learning. Finally, glutamate and GABA levels were correlated during high cognitive load. These results suggest that availability of dACC inhibitory resources enables successful learning. Our approach helps elucidate the potential contribution of the balance between excitation and inhibition to learning and motivation in behaving humans.

1. Introduction

Studies in animals have highlighted the importance of excitation and inhibition for reinforcement learning (Johansen et al., 2011; Kelley, 2004; Myhrer, 2003). The balance between them (E/I balance) is critical and maintained under most conditions, yet the exact ratio is highly dynamic (Isaacson and Scanziani, 2011; Treviño, 2016), and variations in this ratio support information processing and learning (Isaacson and Scanziani, 2011; Letzkus et al., 2011). Although it is much harder to assess excitation and inhibition in humans, the main contributors: Glutamate and GABA, can be measured through Proton Magnetic Resonance Spectroscopy (^{1}H-MRS) (Bottomley, 1987; Mescher et al., 1998; Paul G Mullins et al., 2014). The exact interpretation of MRS-observed neurotransmitter levels remains an open question (Mangia et al., 2007a,b; Stagg et al., 2011). However, both Glutamate and GABA have been shown to reflect task-related activity with studies demonstrating sensitivity to baseline (Donahue et al., 2010; Jocham et al., 2012; Levar et al., 2017; Muthukumaraswamy et al., 2009; Northoff et al., 2007; Yoon et al., 2016) and rapidly-modulating levels (Floyer-Lea et al., 2006; Hasler, van der Veen, Grillon, Drevets and Shen, 2010; Mangia et al., 2007a,b). Most studies measured concentrations during rest and correlated it with later/previous behavior (Boy et al., 2010; Muthukumaraswamy et al., 2009; Northoff et al., 2007; Schmitz et al., 2017; Sumner et al., 2010; Yoon et al., 2016), yet some even measured during behavior (Hasler et al., 2010; Mangia et al., 2007a,b; Michels et al., 2012). A few studies have correlated baseline (rest) levels with subsequent/prior learning metrics (Jocham et al., 2012; Levar et al., 2017; Sampaio--Baptista et al., 2015), and one has even examined changes during motor learning (Floyer-Lea et al., 2006).

Error-based learning involves the dorsal-anterior-cingulate-cortex (dACC), which mediates motivation, cognition and action (Dayan and Niv, 2008; Haber and Knutson, 2010; Heilbronner and Hayden, 2016; Kennerley et al., 2006; Lee et al., 2012). The dACC plays a crucial role in reward-guided decision making, as it promotes action-outcome

* Corresponding authors. 234 Herzel St., Rehovot 7610001, Israel.
E-mail addresses: rony.paz@weizmann.ac.il (R. Paz), assaf.tal@weizmann.ac.il (A. Tal).
[1] These authors contributed equally to the work.

https://doi.org/10.1016/j.neuroimage.2018.09.016
Received 12 May 2018; Received in revised form 10 August 2018; Accepted 7 September 2018
Available online 7 September 2018

associations and monitors goal-directed behaviors (Kennerley et al., 2006; Kolling et al., 2016). In particular, dACC activation is modulated by requirements for cognitive control (Ridderinkhof et al., 2004; Shenhav et al., 2016; Sheth et al., 2012), and is involved in monitoring choice outcome in uncertain environments (Amiez et al., 2005; Behrens et al., 2007; Payzan-LeNestour et al., 2013), as well as biases decisions that require high mental effort (Croxson et al., 2009; Prévost et al., 2010; Rudebeck et al., 2006). Its overall involvement in error detection and processing, as well as conflict monitoring, further link it to learning processes (Botvinick, 2007). There have been several studies which have examined the neurometabolic changes in the dACC during interference and Stroop tasks (Kuhn et al., 2016; Taylor et al., 2015); and the functional metabolic correlates of learning in hippocampal and striatal systems (Bell et al., 2018; Stanley et al., 2017). However, the contribution of excitation-inhibition mechanisms to learning processes in the human ACC remains poorly understood.

In the current study, we used functional ^{1}H-MRS (^{1}H-fMRS) during reinforcement learning in humans, and measured modulations in dACC levels of GABA and Glx while participants engaged in a learning task that compared three factors: full uncertainty (high-cognitive-load); probabilistic discrimination learning, and an active Null condition. Based on prior studies which demonstrated recruitment of the dACC during

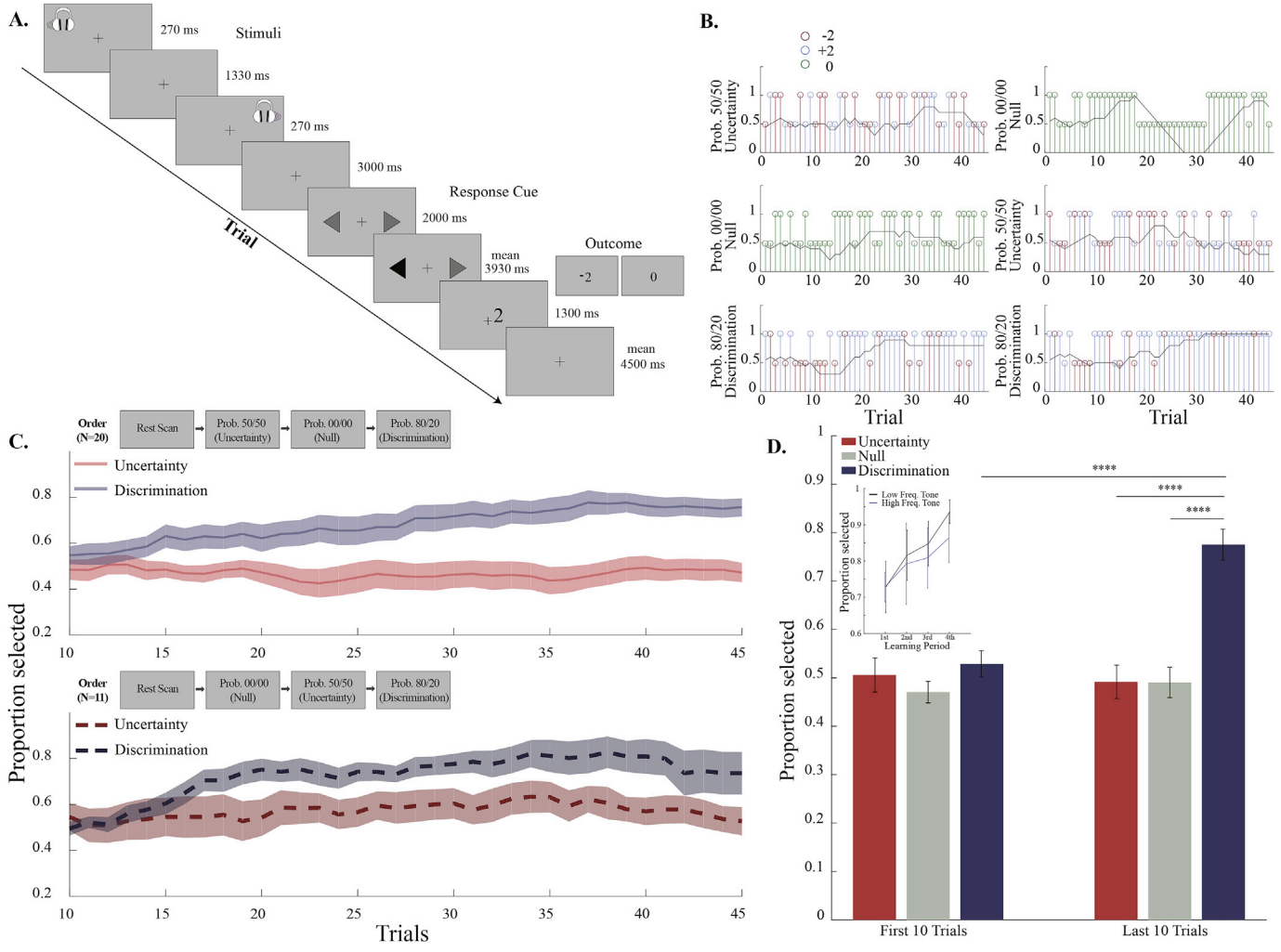

Fig. 1. Experimental design and behavioral results.

A. In each trial, participants were exposed to two pure tones that were played out in succession to different ears. The response cue, presented by two gray opposing arrows, instructed to choose between the tones (left or right button press). Following selection, the arrow corresponding to the chosen laterality was blackened, and the outcome screen indicated monetary gain, loss or neutral outcome (+2,-2 or 0).

B. Behavior of single two participants (rows), in the order of exposure to each of the 3 conditions (rows, top to bottom). The scanning session consisted of three scanning blocks, each attributed to one behavioral condition: 50/50 probability to lose or gain 2₪ ("uncertainty condition"), 00/00 probability with consistent 0₪ reward ("Null condition"), and 80/20 probability to lose or gain 2₪ ("discrimination condition"). Blue, red and green represent gain, loss and zero reward respectively. Taller stems represent selection of one tone, while shorter stems represent selection of the other tone (1 and 0.5 in the y axis respectively). The black line is the probability to choose the tone designated as the gain-tone in the 80/20 condition, averaged over a 10-trial moving window.

C. Tone selection probability during the uncertainty and discrimination conditions, presented separately for the two ordering of conditions (mean ± shaded SEM). Top: average across participants that were exposed to the first ordering (n = 20): MRS rest scan, followed by the uncertainty, Null, and discrimination conditions. Bottom: average across participants that were exposed to the second ordering of conditions (n = 11): MRS rest scan followed by the Null, uncertainty, and discrimination conditions. The graphs demonstrate a gradual increase in the high-gain-tone ('better-option') selection probability during the discrimination condition, irrespective of the ordering, and no selection preference during the uncertainty condition (see text for statistics).

D. High gain tone selection probability averaged across the first and last 10 trials in each condition (mean ± SEM). Participants chose the high gain tone more often in the last part of the discrimination condition compared to its first part, as well as to the last parts of the two other conditions (****$p < 0.0001$, post-hoc Tukey-Kramer). Inset presents pretest results (n = 10) showing that learning was similar regardless of whether a high frequency (light blue) or low frequency tone served as the better-option (Wilcoxon $p > 0.05$ in each one of the four points comparisons).

uncertain choice outcomes and high mental effort, we hypothesized that MRS levels of neurotransmitters during the uncertainty condition, which introduced high cognitive load, would be altered. We set out to test this hypothesis, as well as explore other potential metabolic correlates of E/I balance during learning.

2. Materials and methods

2.1. Participants

All studies were performed in accordance to the procedures approved by the Internal Review Board of Haemek Medical Center (Afula, Israel). Thirty-seven right-handed healthy participants (age range 22–39 years; median age 26 years; 21 females) took part in the experiment after written informed consent was obtained. Three participants were excluded from the experiment due to distorted signals, resulting from magnetic field drift, improper shimming or motion. Three additional participants were excluded due to recurrent GABA and Glx outlier levels (more than 2.5 standard deviations).

2.2. Behavioral paradigm

A two-alternative forced choice task was conducted using a block design paradigm (Fig. 1A), while participants (n = 31) laid in an MRI scanner. During each trial, participants heard two short (270 ms) pure-frequency tones which were played out in succession and in a random order, each to a different ear. Subsequently, a visual response cue appeared, comprised of two arrows, corresponding to the two sides the tones were played to. The participants chose their preferred tone by selection of the right or left remote buttons of a response box, corresponding to the side their preferred tone was played to. Following the selection, the chosen arrow was marked in black and subsequently an outcome screen appeared, presenting the response for the last selection, which was one of three possible outcomes: a monetary gain (+2), loss (−2) or neutral feedback (0). The paradigm consisted of three experimental conditions, each implemented within a separate block composed of 45 trials and lasting 12 min: (1.) the null condition with a consistent 0 reward (00/00 probability of loss/gain); (2.) the uncertainty condition (50/50 loss/gain probability, independent of the participant's choice); and (3.) the discrimination condition (80/20 loss/gain probability), in which one of the tones was paired with a monetary gain in 80% of the trials it was chosen and monetary loss in 20% of the trials it was chosen, and vice versa for the other tone. Stimuli were generated by MATLAB (R2015b, The MathWorks, Natick, USA) using the Psychophysics Toolbox extension (Brainard and Vision, 1997). Each of the conditions was assigned one of three pairs of tone frequencies, mixed between participants in pairing order. The tones' frequencies were kept at a 4:7 ratio to facilitate their distinction. A fourth frequency pair was assigned to a short initial training session.

Pretest A pre-test was conducted prior to the experiment to examine innate bias to low or high frequency tones. We compared between two groups with n = 5 participants each, in one the low frequency tones and in the other the high frequency tone was associated with the higher monetary gain in the discrimination condition (0.8 probability to gain money). The trials were divided into four periods, and the averaged selection probability was calculated for the tone that was associated with higher monetary gain. No bias was evident, and learning was similar to both options (Fig. 1D inset; Wilcoxon $p > 0.05$ in each one of the periods).

2.3. MR scanning protocol

MR data was collected using a 3 T Tim Trio scanner (Siemens, Erlangen), with a 12-channel receiver head coil. Body coil with a peak B_1 of 19 μT was used for transmission. Anatomical images were acquired using three-dimensional T_1-weighted MPRAGE sequence ($1 \times 1 \times 1$ mm^3 voxels, TR/TE/TI = 2300/2.98/990 ms, 176 slices, FA = 9°, in-plane FOV = 256×256 mm^2, TA = 4:44 min). The sagittal and coronal T_1-weighted anatomical images enabled localization of a $40 \times 25 \times 10$ mm^3 ^{1}H-MRS voxel on the midline of the dACC (Fig. 2A). In order to enhance magnetic field homogeneity, first and second order shim adjustments were performed using the default Siemens shimming tool, yielding water line widths of 6–7 Hz. The GABA and Glx ^{1}H-MRS spectra were acquired using the spectral editing sequence Mescher-Garwood Point RESolved Spectroscopy (MEGA-PRESS) (Mescher et al., 1998). Each MEGA-PRESS scanning block (TR/TE = 2000/68 ms, 2048 complex FID points, 2 kHz bandwidth, 16-step phase cycle) consisted of a metabolite scan (144 averages, TA = 9:57 min) that was followed by a water reference scan (16 averages, TA = 1:00 min). Transmitter frequency was set to Creatine's methyl peak at 3 ppm. The individual coils' spectra were phased and weighted by their signal to noise ratios using the reference coil sensitivity maps before combining their respective spectra.

2.4. Procedure

Participants underwent initial training composed of four trials in front of a computer to ensure the task was correctly understood. Upon completion, they entered the magnet head first supine, while being visually monitored for awareness. A response box was handed to all participants, and a projector was used for visual feedback while lying in the scanner. Anatomical images were acquired and enabled localization of the ^{1}H-MRS voxel in the dACC. Shimming was carried out, followed by a ^{1}H-MRS "rest" scan, during which the participants were asked to focus on a fixation cross placed at the center of the screen. Following the rest scan, the participants began the experimental session in which, at the onset of each experimental condition block, a MEGA-PRESS metabolite scan was initiated, followed by a water reference scan. The responses of the participants, along with the rewards they received, were recorded and labeled (Fig. 1B). The participants were divided into two cohorts, each exposed to a different ordering of the experimental conditions (Fig. 1C): The first cohort (20 participants) started with two blocks of the uncertainty condition, continued with one block of the null condition, and concluded with two blocks of the discrimination condition. The second cohort (11 participants) started with one block of the null condition, followed by two blocks of the uncertainty condition and concluded with two blocks of the discrimination condition. Eighteen participants (seven from the first cohort and all participants from the second cohort) also performed an additional and final rest scan after concluding the task.

2.5. Behavioral analysis

The behavioral data was analyzed concentrating on the first block of each condition, using in-house MATLAB scripts. In order to examine the dynamics of the participants' choices over the course of each experimental condition's block, we performed a moving average of the selection probability with a window width of 10 trials. Additionally, to assess behavioral performance per condition, we calculated the averaged selection probability of the high gain tone. To probe the learning rate in the discrimination condition, we calculated the mean overall selection probability, and used the first trial in which each participant reached this selection probability. Two participants didn't reach the learning rate criterion of 0.7 and therefore were eliminated from this analysis.

2.6. 1H-MRS processing and quantification

MEGA-PRESS spectra were analyzed using in-house MATLAB scripts. Spectra were zero-filled 8-fold, apodized using an exponentially time decaying function with a linewidth of 3.2 Hz, Fourier transformed and phased. Frequency alignment was carried out shot-by-shot using the NAA's methyl singlet at 2.01 ppm. Difference spectra were generated by subtraction of the alternating ON and OFF spectra.

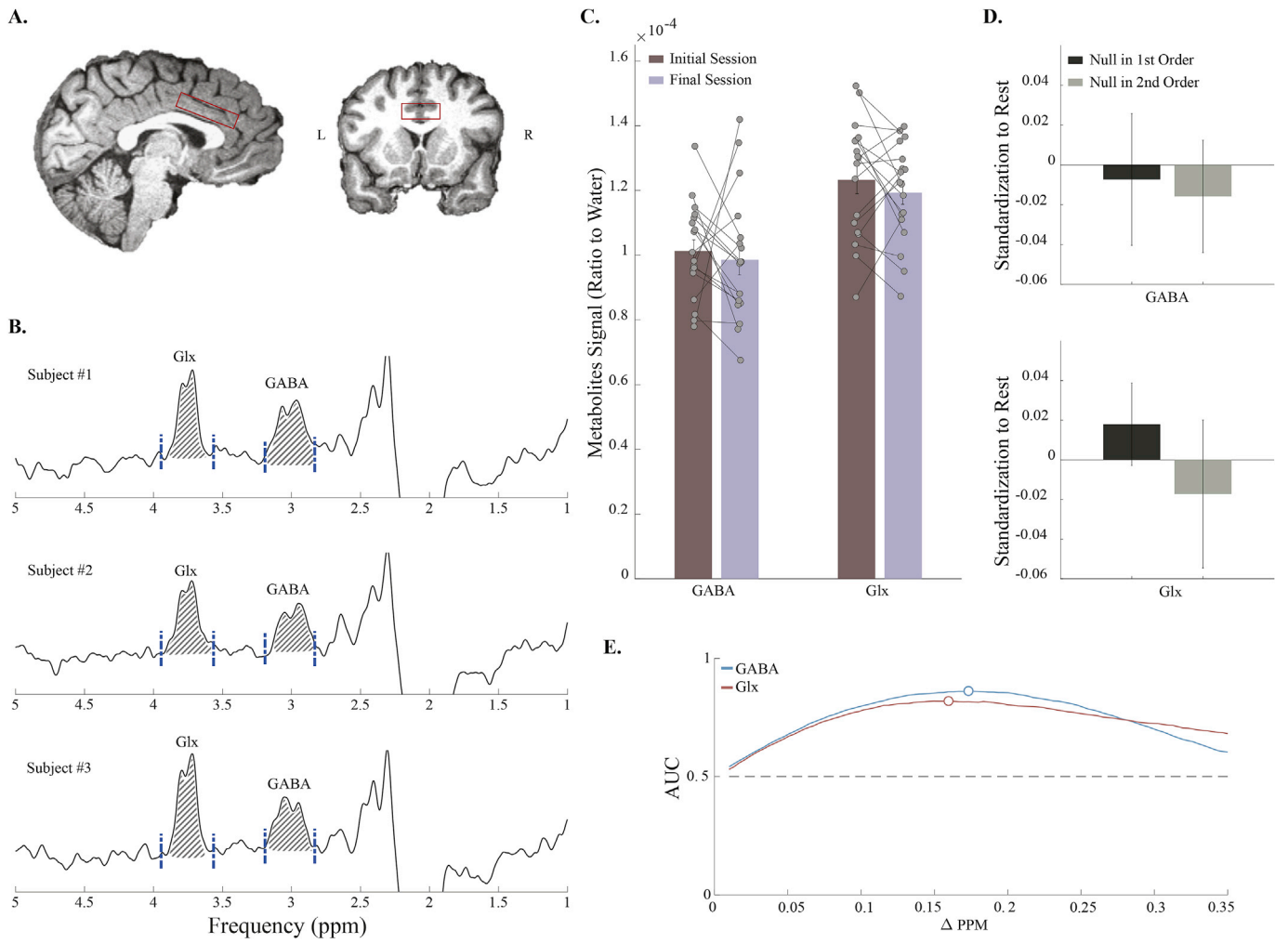

Fig. 2. MRS measurements of GABA and Glx concentrations are stable.

A. A $40 \times 25 \times 10\,mm^3$ voxel was placed on the midline of the dACC, chosen anatomically, presented in sagittal (left) and coronal (right) T1-weighted anatomical MPRAGE scans.

B. Sample spectra from three different participants (144 averages, 9:57 min), displaying the peaks of GABA and Glx at 3.01 and 3.75 ppm respectively. Blue dashed lines represent the integration limits that were used to quantify each metabolite. The integrated area under the curve, used for quantification, is illustrated by diagonal lines.

C. Eighteen participants went through an additional final session of rest scan after completion of the task. Comparison between metabolites levels in the initial and in the final rest scans, revealed no difference over time in GABA/Water and Glx/Water levels ($p > 0.05$, paired sample *t*-test). Levels of metabolites in single participants are represented by connected dots (mean ± SEM).

D. Order of experimental conditions did not affect metabolite levels in the Null condition. Compared between the first (n = 20) and the second (n = 11) orderings for both GABA and Glx standardized to rest (Wilcoxon $p > 0.05$). (mean ± SEM).

E. Chosen integration limits for each metabolite were validated to be robust by an optimization process. We varied the limits and used an ROC curve analysis to choose the best limits. Shown are area-under-curve (AUC) for the tested integration limits of Glx and GABA, with the best integration limits for each metabolite circled in blue. Delta PPM denotes integration limits width around each metabolite peak. The gray dashed line denotes chance level. The results are highly similar to the limits chosen traditionally (usually based on visual considerations alone).

Metabolite quantification was achieved via peak integration with the integration limits 3.59 to 3.94 for Glx and 2.84 to 3.20 for GABA (Fig. 2B). The signals of GABA's methylene group + macromolecular contributions at 3.01 ppm (De Graaf, 2013; Paul G Mullins et al., 2014), and the Glx complex at 3.75 ppm are represented by:

$$S \propto C \cdot V \cdot (1 - f_{CSF}) \cdot B_{1-} \cdot f_R$$

where C is the metabolite's concentration, V the voxel volume, B_{1-} the receiver coil sensitivity, f_{CSF} the fraction of CSF in the voxel, and f_R a factor accounting for T_1 and T_2 relaxation. Taking the ratio of each metabolite to the reference water signal (GABA/water, Glx/water) removed common factors such as B_{1-} and V, and reduced signal variability. The remaining factors, such as f_R and f_{CSF}, as well as the macromolecular contamination, remained unaccounted for, but were assumed constant throughout the paradigm when interpreting our results. Since our analysis focused on intra-subject changes to metabolite levels during the learning task, these inter-subject sources of variability did not bias our conclusions. To further factor-out these constant elements we have also examined the standardized differences:

$$f^{met}_{A,B} = \left(\frac{S^{met}_A}{S^{water}_A} - \frac{S^{met}_B}{S^{water}_B}\right) \Big/ \left(\frac{S^{met}_A}{S^{water}_A} + \frac{S^{met}_B}{S^{water}_B}\right), \quad (1)$$

where *met* = Glx, GABA and A,B = null, discrimination, uncertainty or rest. The expression in Eq. (1) is independent of f_{CSF}, f_R, B_{1-} and any other factor assumed unchanged between conditions. This expression, when standardized to rest, served as standardization to baseline activity,

and when was conducted between two conditions was reflecting a direct comparison between conditions of the task.

For inter-subject correlations and comparison, tissue fraction corrections were applied using SPM12 (Wellcome Trust Center for Neuroimaging; http://www.fil.ion.ucl.ac.uk/spm/): The structural MPRAGE images were segmented into white matter (WM), gray matter (GM) and cerebrospinal fluid (CSF) maps, and their fractions within the MRS voxel, f_{GM}, f_{WM}, f_{CSF} were calculated using in-house software. These were used to apply tissue content correction to the metabolites' concentrations as described elsewhere (Gasparovic et al., 2006).

2.7. Setting the integration limits

To fix the integration limits for each metabolite, limits were varied from 3.01 ± 0.01 to 3.01 ± 0.35 ppm for GABA and 3.755 ± 0.01 to 3.755 ± 0.35 ppm for Glx. For each integration interval, simulated GABA and Glx resonances were generated for both a rest condition and an activated condition, assumed to correspond to GABA and Glx levels elevated by 10%. A simulated cohort of $N_{sub} = 30$ participants was created for each of the conditions using the simulated spectra with added white noise corresponding to the actual noise observed in the measurement for GABA (SNR = 12). A paired *t*-test was used to determine whether differences were observed between the activated and rest conditions, as well as between two separate rest conditions, with $\alpha = 0.05$ significance. This was repeated using a Monte-Carlo simulation with $N_c = 10{,}000$ cohorts to calculate the fraction of false positives and true positives, which were used to construct the receiver operating characteristic (ROC) curve for our chosen integration limits. The area under the curve (AUC) was calculated for each integration limit, and the integration limits having the highest AUC were chosen for each metabolite. We note that the process resulted in integration limits that are highly similar to the ones chosen by an experienced observer and/or in similar studies that set such limits a-priori.

2.8. Statistical tests

Changes to within-subject behavioral and metabolic measures were compared using two- or one-way repeated measure analyses. Tucky-Kramer tests were conducted for post-hoc paired comparisons. One sample t-tests was conducted in order to assess normalized metabolic levels significance, while paired sample t-tests was conducted for temporal metabolic drift analysis. Additionally, in order to further analyze metabolic drift, Bayes factor was calculated using JASP (Version 0.9.0.1; JASP team, 2018). The Bayes factor quantifies evidence regarding two competing models (null and alternative hypothesis) and is used to compare the relative predictive adequacy of the two (Wagenmakers et al., 2018). To analyze behavioral pretest data and in order to assess conditions ordering effect, we performed unpaired group comparisons using nonparametric Wilcoxon rank sum tests. Pearson's correlation coefficient was conducted in order to test correlations between metabolites levels and behavioral performance. Unless otherwise stated, significance level was set to $P < 0.05$.

3. Results

3.1. MRS metrics and integration limits

The SNR per condition in the unapodized OFF spectrum for the NAA 2.01 ppm methyl group was 62 ± 4 (mean ± s.d., taken over all participants). GABA SNR in the apodized difference spectra was 12 ± 3. Frequency drifts and phase fluctuations were minimal throughout, with $\Delta\nu = -0.9 \pm 0.6$ Hz and $\Delta\phi = -2.3° \pm 1.4°$ per condition, indicating a high degree of stability throughout. Since our phase correction algorithms exhibit similar magnitude errors when applied to spectra with similar SNR, phase correction was not applied to the (already well-phased) data. Our Monte-Carlo ROC curve simulations indicated the AUC is maximized when the integration limits are set to 3.01 ± 0.18 ppm for GABA and 3.755 ± 0.171 ppm for Glx (Fig. 2E). These are similar to the integration limits a human operator would set visually, near the peaks' baseline.

3.2. Learning occurs under probabilistic discrimination, but not under uncertainty or null

Over the course of the discrimination block, participants gradually increased their preference to the tone that was associated with higher gain ('better-option'), such that by the end of this block, the mean selection probability exceeded 70% (Fig. 1B and C). In comparison, no preference to either one of the options was observed during the other two conditions, in which the participants presented a stable mean probability of 0.5 ± 0.04 (uncertainty condition) and 0.48 ± 0.03 (null condition) to select each option (Fig. 1B and C). This was the case for both groups of participants, when the uncertainty condition was first (Fig. 1B-left, Fig. 1C-top, n = 20), and when the Null condition was first (Fig. 1B-right, Fig. 1C-bottom, n = 11).

The preference to the better-option in the discrimination condition was also reflected by the averaged selection probability during two epochs, namely, the first and last 10 trials of the block (Fig. 1D). A difference in selection probability between conditions was observed ($p < 0.00001$, $F(2, 60) = 18.3$, two way repeated measures ANOVA; mean selection probability of the first and second epochs: 0.5, 0.48 and 0.65, in uncertainty, null and discrimination conditions, respectively), arising from a significant preference to the better-option in the discrimination condition when compared to the uncertainty and null conditions ($p < 0.001$ and $p < 0.00001$ respectively, post hoc Tukey-Kramer). Additionally, we also observed a difference between the first and second epochs ($p < 0.001$, $F(1, 30) = 19.2$, two way repeated measures ANOVA) that originated from a preference to the better-option in the second epoch ($p < 0.001$, post hoc Tukey-Kramer). An interaction between these effects was observed ($p < 0.0001$, $F(2, 60) = 12.2$, two way repeated measures ANOVA), deriving from the increased preference to the higher gain tone in the second epoch of the discrimination condition compared to its first epoch ($p < 0.00001$, post hoc Tukey-Kramer). Examination of the performance in the second epoch revealed a preference to the high-gain-tone in the discrimination condition compared to the null and uncertainty conditions (both $p < 0.00001$ post hoc Tukey-Kramer). However, there was no difference in the average selection probability between the conditions in the first epochs of the blocks ($p > 0.05$, post hoc Tukey-Kramer).

We conclude that participants learned the task in the probabilistic discrimination condition, behaved at chance level in the Null condition (no outcomes), and also behaved at chance level under uncertainty (when rewards and punishments occur, but there is no reliable information to learn, leading to a high-cognitive-load).

3.3. Measuring neurotransmitter concentrations in the dACC using ^{1}H-MRS

The MRS technique requires long scanning sessions in order to achieve good signal to noise ratio. Therefore, we defined the region-of-interest (the dACC) a-priori based on anatomical maps (Fig. 2A). Please see methods for full description of how we measure and quantify GABA and Glx concentrations (Fig. 2B). In addition, we conducted two tests to assess whether results might be confounded by the order of experimental conditions and/or the stability of metabolite levels over the long scanning time.

First, we assessed putative temporal metabolic drift by examining metabolites levels during the rest scan, which is the only scan type that was not influenced by task manipulation but could be affected by time. Metabolites levels were compared in participants that performed the rest scan block twice: at the beginning and at the end of the experiment (Fig. 2C, n = 18). There was no difference between the levels of GABA/

Water (t (17) = 0.45, p = 0.66, paired sample *t*-test) or Glx/Water (t (17) = 1.02, p = 0.32, paired sample *t*-test). To further assess the strength of this finding (Wagenmakers et al., 2018) we conducted bayes factor analysis. The bayes factor, expressed as BF_{01}, grades the intensity of the evidence for null hypothesis comparing to the alternative hypothesis, meaning the lack of difference between the levels of the metabolites versus the evidence for a significant temporal metabolic drift. BF_{01} of 3.758 (BF_{10} of 0.266) and 2.612 (BF_{10} of 0.383) were found for the difference between the levels of GABA/Water and Glx/Water respectively. These results indicate the observed data is 3.758 and 2.612 times more likely under the null hypothesis than under the alternative hypothesis for GABA/Water and Glx/Water respectively. We conclude that the time did not influence metabolite levels and is not a major contributor to the results.

To further validate that the order of conditions was not a factor, we compared levels of GABA and Glx during the Null condition between the two groups of experimental order: one group performed the uncertainty condition before the Null condition (n = 20), and the other performed the Null condition before the uncertainty condition (n = 11). Because we already established that metabolite levels during rest are stable from start to end, we standardized GABA and Glx levels during the Null condition to the initial rest level (Eq. (1)). We found no difference (Fig. 2D) between

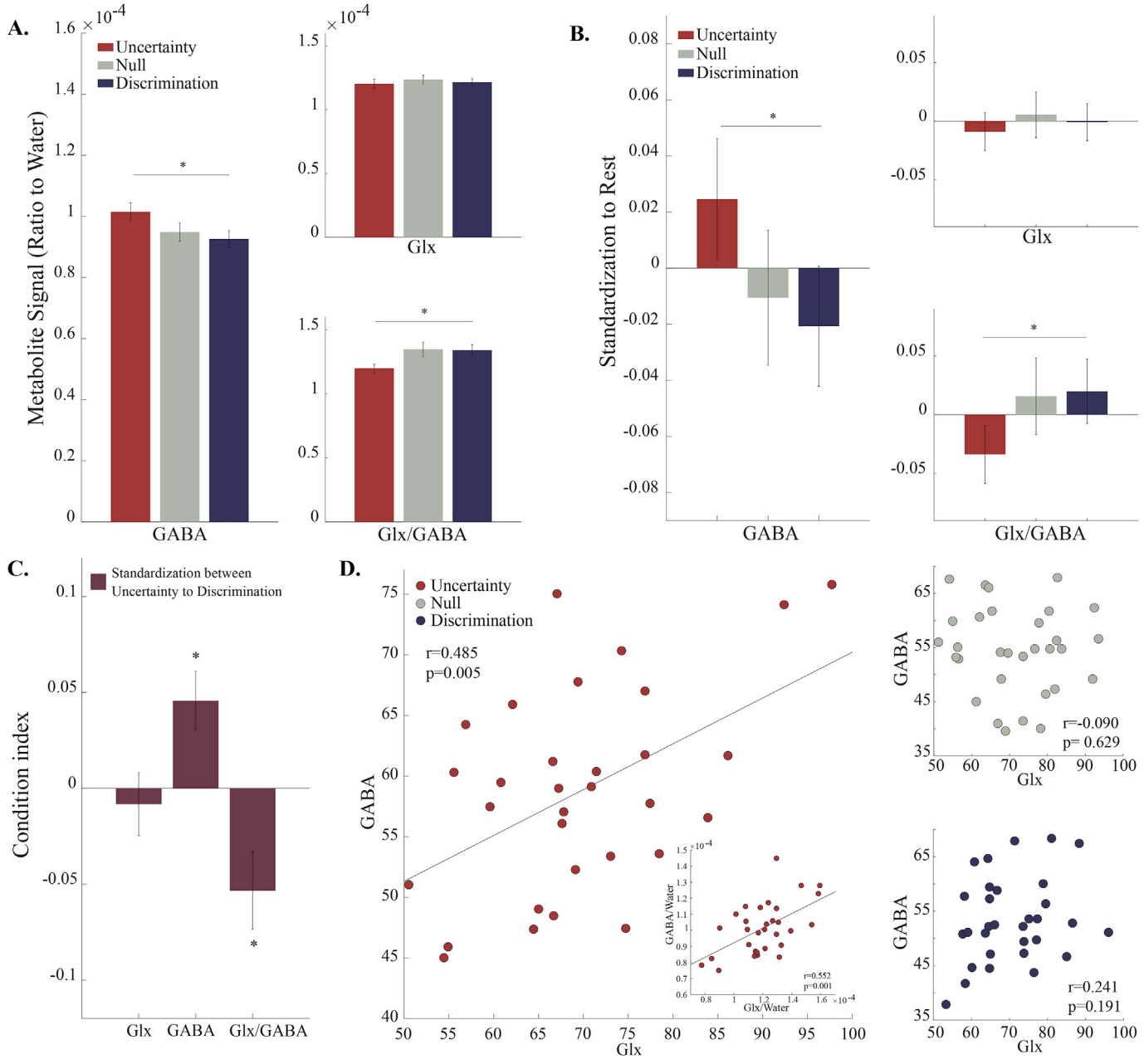

Fig. 3. Higher GABA levels observed during the uncertainty condition.

A,B, Metabolites levels quantified as ratio to water (A) or standardized to rest (B) reveal a consistent result: higher GABA levels and lower Glx/GABA levels in the uncertainty condition, yet lower levels during the Null and discrimination conditions ($p < 0.05$, repeated measures one way ANOVA; $^*p < 0.05$, post hoc Tukey-Kramer). See text for detailed statistics.

C. Standardization between pairs of task conditions reveal significant differences in GABA and Glx/GABA levels when comparing between the uncertainty and the discrimination conditions ($^*p < 0.015$, one sample t-tests with Bonferroni adjusted alpha; error bars represent the SEM).

D. A positive correlation between Glx and GABA levels during the uncertainty condition only ($r=0.485$, $p=0.005$). Inset shows the same with normalization by water signal ($r=0.552$, $p=0.001$).

the signals of GABA (Wilcoxon $p > 0.05$, $Z = 0.18$) or Glx (Wilcoxon $p > 0.05$, $Z = 0.64$).

3.4. Increased GABA during uncertainty condition only

Differences between the conditions of the task were found when examining GABA/Water and Glx/GABA levels (Fig. 3A; $p < 0.05$ with $F(2, 60) = 3.4$ and $F(2, 60) = 3.7$ respectively, one way repeated measures ANOVA). These differences originated from elevated GABA/Water and reduced Glx/GABA levels during the uncertainty condition compared to the discrimination condition ($p < 0.05$, post hoc Tukey-Kramer). Glx/GABA displayed a marginal non-significant trend for the difference between the Null condition to the uncertainty condition ($p = 0.08$, post hoc Tukey-Kramer), but not for GABA/Water levels ($p > 0.1$, post hoc Tukey-Kramer). No differences were found for GABA/water and Glx/GABA between the Null and discrimination conditions ($p > 0.1$, post hoc Tukey-Kramer). Finally, Glx/Water did not exhibit any differences between the conditions ($p > 0.1$, $F(2, 60) = 0.3$, one way repeated measures ANOVA).

To investigate metabolite changes relative to rest, we repeated these comparisons after standardizing Glx, GABA and Glx/GABA to their levels at rest (Eq. (1)). This yielded similar results to the ones obtained using the raw data, mainly presented a significant difference between the uncertainty to the discrimination condition in GABA and in Glx/GABA levels. When standardized to rest, GABA and Glx/GABA levels were found to vary significantly between the uncertainty and discrimination conditions (Fig. 3B; $p < 0.05$ with $F(2, 60) = 3.3$ and $F(2, 60) = 3.4$ respectively, repeated measures one way ANOVA; $p < 0.05$, post hoc Tukey-Kramer). No difference was found between the uncertainty and Null conditions nor between the Null condition and the discrimination condition in GABA levels or Glx/GABA levels ($p > 0.05$, post hoc Tukey-Kramer). Finally, no difference was found between the conditions in Glx levels ($p > 0.05$, $F(2, 60) = 0.4$, one way repeated measures ANOVA).

Furthermore, we standardize directly between conditions (see methods), and used one sample *t*-test with Bonferroni adjusted alpha level of 0.015 (0.05/3). The comparison between the uncertainty to the discrimination condition (Fig. 3C) yielded a significant standardized GABA and Glx/GABA scores ($t(30) = 3.0$, $p = 0.006$, and $t(30) = -2.64$, $p = 0.013$, respectively; one sample *t*-test). As expected, Glx did not change significantly in this comparison ($t(30) = -0.50$, $p > 0.015$, one sample *t*-test). The comparisons between the null to the uncertainty condition and between the null to the discrimination condition were non-significant in all measurements ($p > 0.015$, one sample *t*-test).

It was tempting to hope that Glx/GABA results have an additional component to the GABA findings alone, thereby providing evidence to a specific E/I balance mechanism. To assess whether the significant differences in Glx/GABA between the uncertainty and the discrimination conditions could be explained by GABA, Glx or their combined effect, we implemented repeated measures ANOVA on GABA/water with and without Glx/water as a varying covariate. The resulting effect size increased from $\eta^2 = 0.236$ without the covariate to $\eta^2 = 0.25$ with the covariate. Subsequently, the square of each effect size was modeled as an index of correlation between the learning conditions to the GABA measurement, and a test for the difference between correlations was performed on the Fisher-transformed correlations. The test revealed no difference between correlations, meaning Glx measurement was not found to add any significant information ($Z = 0.056$, $p > 0.05$). We conclude that the major changes between conditions occur due to changes in GABA concentrations mainly.

Our normalized results show changes of metabolites relative to rest, facilitating comparison between the various conditions. However, for the sake of completeness, the full unnormalized results compared to rest scan are provided in the Supplementary Material (S.1.).

3.5. GABA and Glx levels are correlated during uncertainty condition

Although Glx was not found to significantly contribute to the differences observed between the conditions in Glx/GABA, and these were driven mainly by GABA changes – we aimed to further analyze the relationships between Glx and GABA. To do so, we calculated Pearson's correlation coefficient between Glx and GABA in each of the conditions (Fig. 3D). A positive correlation was found during the uncertainty condition ($r = 0.485$, $p = 0.005$), but not during the Null ($r = -0.09$, $p > 0.05$) or discrimination ($r = 0.241$, $p > 0.05$) conditions. This persisted when examining the correlation between GABA/Water and Glx/Water in the uncertainty condition (Fig. 3D inset $r = 0.552$, $p = 0.001$), and again there were no significant correlations in the other two conditions ($p > 0.05$ in both, $r = 0.031$ for Null condition; $r = 0.245$ for discrimination condition). A regression of GABA on Glx levels showed that although they increased in correlation, the E/I balance does change ($\beta = 0.4535$, significantly different than 1, $p < 0.01$). We note that, in general, although the water-normalized GABA/Water and Glx/Water are more indicative of true metabolite concentrations, division by a common reference signal actually increases correlations between the two artificially. We have chosen to present both the normalized and unnormalized levels for the sake of completeness, but caution against blind acceptance of correlations of water-referenced quantities.

We propose that changes in Glx, although too small to show significant variations across conditions, still maintain a balance with the GABA signal when it varies extensively and significantly i.e. when GABA levels are especially high as in the uncertainty condition.

3.6. GABA levels in the Null condition predict learning performance

We tested whether GABA and Glx levels during each experimental condition were directly related to participants' behavioral performance during the discrimination condition, as a proxy for their learning ability (Fig. 4A). To do so, we calculated Pearson's correlation coefficients between the behavioral measures during the discrimination condition to GABA/water and Glx/water levels during the different conditions.

We used two behavioral measures. First, we approximated the learning-rate as the trial when a participant reached performance criterion of 0.7, which is similar to the overall mean selection probability (0.69). There was a negative correlation (Fig. 4B) between the learning-rate and GABA/water levels during the Null condition ($r = -0.592$, $p < 0.001$), but not during the discrimination ($r = -0.040$, $p = 0.827$) or uncertainty ($r = 0.082$, $p = 0.672$) conditions. Glx/water levels in the different experimental conditions did not reveal significant correlations with learning rate ($p > 0.05$ in all conditions, $r = -0.06$ for Null condition; $r < 0.001$ for uncertainty condition; $r = -0.2$ for discrimination condition).

Second, we assessed behavioral performance by the proportion of selection of the better-option. We found a positive correlation (Fig. 4C) between the proportion of selection and GABA/water levels during the Null condition (Fig. 4C; $r = 0.444$, $p = 0.012$); but not during the other two conditions ($r = 0.013$, $p = 0.941$ for uncertainty; $r = 0.081$, $p = 0.664$ for discrimination). As before, the selection probability was uncorrelated with Glx/water levels in any of the conditions ($p > 0.05$ in all conditions; $r = 0.02$, 0.10 and 0.18 for the null, uncertainty and discrimination conditions, respectively).

We conclude that baseline levels of available GABA, i.e. in a Null condition, predict better performance in a subsequent discrimination learning task.

4. Discussion

Using fMRS in conjunction with the presented behavioral paradigm has allowed us to examine excitatory and inhibitory modifications to the dACC during learning. Behaviorally, the participants performed the task as expected, and learned to prefer the option that predicted higher gain in the discrimination condition, while lacked any preference in the two other conditions. Increased GABA and decreased Glx/GABA levels were observed during the uncertainty condition, when rewards and

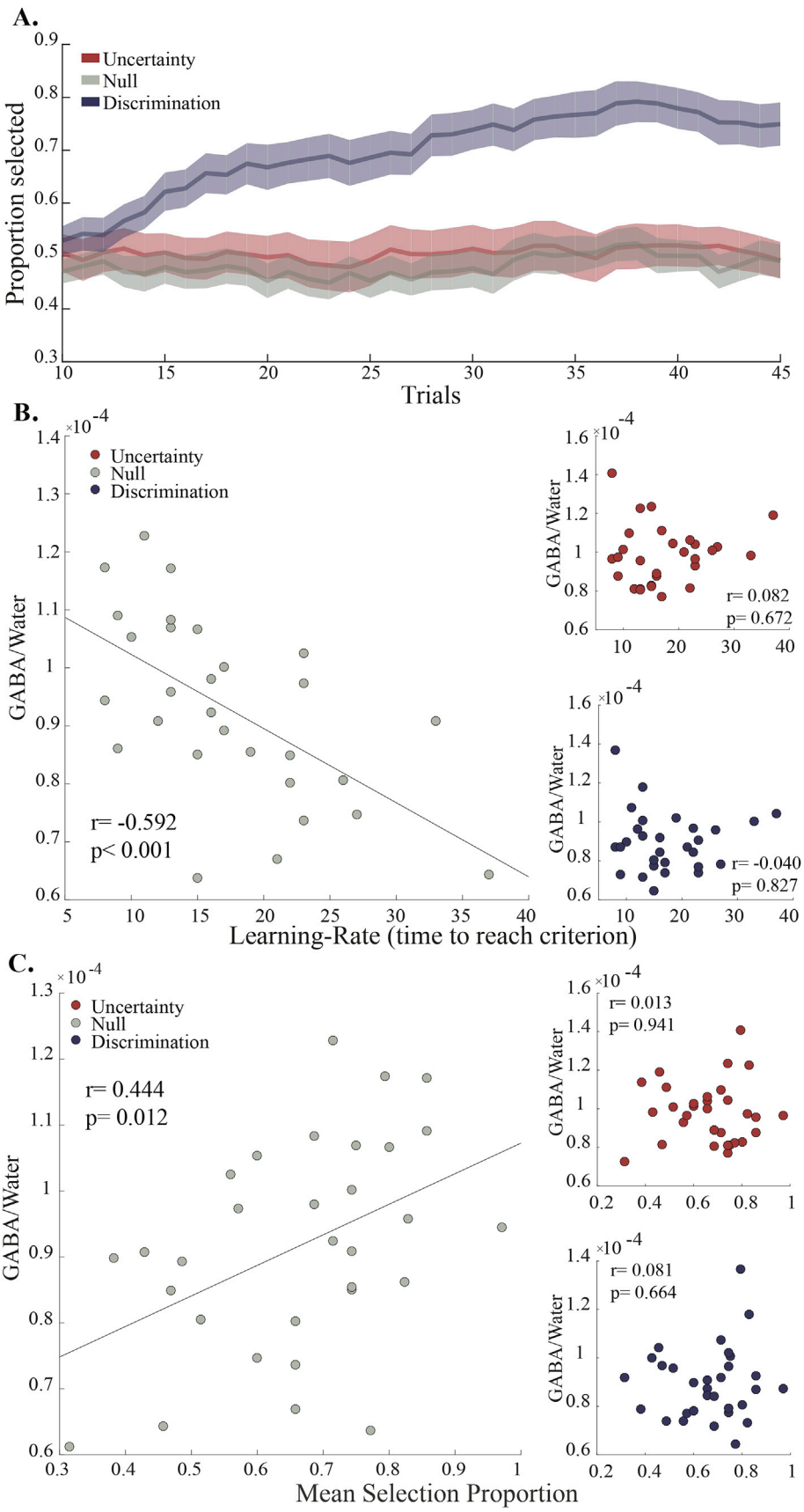

Fig. 4. GABA levels in the Null condition predict behavioral performance during discrimination learning condition.

A. Behavioral performance across all conditions. Gradual increase in selection probability of the better-option (high-gain tone) is observed during the discrimination condition. Averaged across all participants (n = 31) in 10-trial running window (mean ± SEM).

B. Negative correlation between the learning-rate, quantified as the trial # when a 0.7 criterion is reached during the discrimination condition, and GABA/water levels during the Null condition (*r=-0.592, p < 0.001*).

C. Positive correlation between mean selection of the better-option during the discrimination condition and GABA/water levels during the Null condition (*r=0.444, p=0.012*).

punishments are abundant, but there is no information to learn from. Although Glx was not significantly altered across conditions and did not seem to contribute beyond GABA to the difference in Glx/GABA across the conditions, further analysis revealed that Glx and GABA were positively correlated in the uncertainty condition only. This supports the notion that excitation/inhibition balance is maintained, such that changes to GABA are matched by changes to Glx. It is our interpretation that this occurs throughout the experiment, but that only the uncertainty condition has triggered sufficiently large changes for this to be observed. Finally, examination of the relationship between GABA levels to the behavioral measures revealed that higher GABA levels in the Null condition predicted better learning, both when measured as time to reach criterion (learning rate), and when measured as final performance. There have been multiple publications linking basal GABA levels to behavioral metrics (Levar et al., 2017; Schmitz et al., 2017; Sumner et al., 2010); our result, in conjunction with the fact that resting levels of GABA and Glx did not correlate with any behavioral metric (see Supplementary Material), suggests that an active null condition, which factors out the subject's behavior (sans learning), is a more correct predictor of learning performance. This should be considered when designing future experiments.

As previously shown, E/I balance is essential for cortical network stability (Isaacson and Scanziani, 2011; Treviño, 2016; Van Vreeswijk and Sompolinsky, 1996; Yizhar et al., 2011). The precision of the balance depends on the degree of correlation between excitation and inhibition, ranging from a global balance in the absence of correlated inputs to a detailed balance for strong correlations (Vogels et al., 2011). The tight correlation, observed during the uncertainty condition, suggests a more homeostatic activity, in which specific functional patterns are amplified (Murphy and Miller, 2009) and promote the occurrence of a distinctive functional activity. Moreover, we observed elevated GABA levels that can be interpreted as increase in inhibition which occurred in situations that are known to modulate the activity of the dACC, and consist of uncertain rewards (Amiez et al., 2005; Behrens et al., 2007; Payzan-LeNestour et al., 2013; Walton et al., 2007), high mental effort (Croxson et al., 2009; Hosking et al., 2014; Prévost et al., 2010; Rudebeck et al., 2006), and requirements for cognitive control (Ridderinkhof et al., 2004; Shenhav et al., 2016; Sheth et al., 2012). Additionally, a line of evidence linked the inhibitory system with achievement of efficient performance during high cognitive load (Aron, 2007; Medalla and Barbas, 2009). Therefore, presumably, during a need to make a decision in highly demanding cognitive load, specific functional patterns are amplified in the dACC and an increased inhibition occurs. This inhibition is required in order to achieve efficient and better performance. Similarly, individual differences in inhibition levels in the dACC might be linked to each individual experienced cognitive load, and reflect mental effort, uncertainty or a need for cognitive control.

In a neutral situation, such as the Null condition, the influences of external cognitive aspects of learning like incentives (rewards/punishments) are likely eliminated, exposing the underlying intrinsic attention-oriented processes, or simply the availability of the relevant neurotransmitter. Therefore, the correlation between inhibition in the dACC during neutral situation and later performance when learning is possible, might reflect the connection between the cognitive load and the motivational processes that take place during learning (Anselme, 2010; Braver et al., 2014; Etzel et al., 2015; Shenhav et al., 2013), which in their turn, lead to a better performance (Cerasoli et al., 2014). The fact that we did not identify any changes during learning itself (the discrimination condition) remain to be explored further. A possible interpretation is that learning occurred too fast for the long scan process required for MRS to detect changes beyond the signal-to-noise ratio. Fig. 1C reveals learning plateaus approximately mid-way throughout the block. This could be ameliorated in future studies by further fine-tuning the learning probabilities, slowing down the learning rate, or by considering other, event-related fMRS designs (Apsvalka et al., 2015; Gussew et al., 2010; Lally et al., 2014). Yet another possibility is that once uncertainty is reduced (because the participants unveil a pattern to learn), less and less inhibitory mechanisms are required to maintain high cognitive load, attention, or uncertainty. A final possibility we cannot rule-out is that the number of errors as well as punishments diminishes quickly, and the dACC signal diminishes with it.

Overall, the effects demonstrated here emphasize the importance of the dACC in processes of decision making and expand the understanding regarding its involvement in high cognitive demanding situations, and how it can later enable better learning. Importantly, it supports the further use of MRS in behavior and cognition, as a tool for identifying specific neural mechanisms which alter neurotransmitter levels in brain networks during active behavior. The next steps should examine further regions, either by a-priori selection as done here, or by development of better sequences that allow simultaneous measurements from several regions. Combined with the paradigm we used here, it helps elucidate the contribution of excitatory and inhibitory modifications during active learning in humans.

4.1. Caveats

While MRS can directly detect the signals of GABA and glutamate, several of its shortcomings should be noted. Both metabolites' signals are contaminated: GABA contains contribution from additional macromolecules present at 3.0 ppm, which account up to approximately 40% of GABA's signal (Kegeles et al., 2007). Glutamate's signal contains a smaller contribution from glutamine at approximately a 4:1 ratio (Ramadan et al., 2013), and, although there have been recent reports investigating their potential separation at 3T (Sanaei Nezhad et al., 2018), the current study, while relies on peak integration, reports their combined signal, Glx. It should be noted that there is no a-priori reason to expect macromolecules and other contaminants to significantly change during activation, which means alterations to GABA levels do correspond to changes to GABA itself, although this hypothesis remains to be tested.

The interpretation of the MRS signals is a topic of ongoing debate, and care should be taken when specifically linking metabolite levels to neuronal activation and neurotransmitter release. Several previous fMRS works which focused on non-edited sequences and reported alterations to Glutamate, Lactate and Acetate levels have suggested alterations to Glu reflect activity of the malate-aspartate shuttle, i.e. cellular energetics (Bednarik et al., 2015; Mangia et al., 2003, 2009). Others have used the echo-time dependence of the fMRS Glu signal to argue in favor of a more direct association between it and synaptic glutamate (P. G. Mullins, 2018). Again, it is yet unclear whether certain pools, such as the highly concentrated semi-solid glutamate embedded in the gel matrices found within synaptic vesicles, are even MR-visible. Changes to GABA levels are similarly difficult to interpret, with some studies linking MRS GABA to extracellular tonic as well as short interval cortical inhibition using transcranial magnetic stimulation (Stagg et al., 2011). It could also be claimed that GABA acts as a surrogate marker for glutamate, its precursor, which could be related to our observed correlation between GABA and Glx during the uncertainty condition, although it is unclear to which extent.

No additional BOLD fMRI data was acquired from our participants due to time constraints. We've relied on the preponderance of evidence (Ridderinkhof et al., 2004) implicating the dACC in multiple tasks involving decision uncertainty, pre-response conflict, response error and reward mechanisms, all of which are recruited during the current paradigm. However, the lack of an additional BOLD acquisition also indicate our metabolite levels could not be correlated to the dACC's hemodynamic response, a topic that awaits further investigation. Furthermore, we did not account for BOLD effects on the spectroscopic signals, due to the study design employed: metabolite levels were compared during three conditions, all of which involved some form of activation of the dACC (null, uncertainty, discrimination). It could also be argued that, even when comparing levels to rest, but unlike echo based gradient-echo sequences, BOLD only alters metabolite signals minimally: integration of

the peaks removes any T_2 and T_2* dependence of the signal during its free induction decay. MEGA-PRESS acquires a spin-echo signal with $\exp\left(-\frac{TE}{T_2}\right)$, and any BOLD-related alterations to T_2 (not T_2*) will be reflected through that. Spin-echo BOLD effects tend to be very small, on the order of several milliseconds. Typical GABA T_2s are on the order of 90 ms. If we assume a 1% change from $T_2^{rest} = 90$ ms to $T_2^{act} = 91$ ms during BOLD, this would alter the weighting from $\exp\left(-\frac{TE}{T_2^{rest}}\right) \Big/ \exp\left(-\frac{TE}{T_2^{act}}\right) = 0.991$ (using TE = 68 ms), under 1%. This is significantly smaller than the changes to GABA observed during the uncertainty condition, which are on the order of 5–10%. Even smaller effects are expected for Glx, which has longer T_2s. Indeed, if BOLD signal changes to either water or metabolite signals would have been a major contributing factor, this would have been observed for Glx.

Acknowledgments

We thank Dr. Edna Furman-Haran, Nachum Stern and Fanny Attar for assisting with the MRI procedures. This work was supported by ISF #26613 and ERC-2016-CoG #724910 grants to R. Paz, and the Minerva Foundation for A. Tal. A. Tal also acknowledges the support of the Monroy-Marks Career Development Fund and the historic generosity of the Harold Perlman Family.

Appendix A. Supplementary data

Supplementary data related to this article can be found at https://doi.org/10.1016/j.neuroimage.2018.09.016.

References

Amiez, C., Joseph, J.-P., Procyk, E., 2005. Reward encoding in the monkey anterior cingulate cortex. Cerebr. Cortex 16 (7), 1040–1055.
Anselme, P., 2010. The uncertainty processing theory of motivation. Behav. Brain Res. 208 (2), 291–310.
Apsvalka, D., Gadie, A., Clemence, M., Mullins, P.G., 2015. Event-related dynamics of glutamate and BOLD effects measured using functional magnetic resonance spectroscopy (fMRS) at 3T in a repetition suppression paradigm. Neuroimage 118, 292–300. https://doi.org/10.1016/j.neuroimage.2015.06.015.
Aron, A.R., 2007. The neural basis of inhibition in cognitive control. Neuroscientist 13 (3), 214–228.
Bednarik, P., Tkac, I., Giove, F., DiNuzzo, M., Deelchand, D.K., Emir, U.E., Mangia, S., 2015. Neurochemical and BOLD responses during neuronal activation measured in the human visual cortex at 7 Tesla. J. Cerebr. Blood Flow Metabol. 35 (4), 601–610. https://doi.org/10.1038/jcbfm.2014.233.
Behrens, T.E., Woolrich, M.W., Walton, M.E., Rushworth, M.F., 2007. Learning the value of information in an uncertain world. Nat. Neurosci. 10 (9), 1214.
Bell, T., Lindner, M., Mullins, P.G., Christakou, A., 2018. Functional neurochemical imaging of the human striatal cholinergic system during reversal learning. Eur. J. Neurosci. 47 (10), 1184–1193. https://doi.org/10.1111/ejn.13803.
Bottomley, P.A., 1987. Spatial localization in NMR spectroscopy in vivo. Ann. N. Y. Acad. Sci. 508 (1), 333–348.
Botvinick, M.M., 2007. Conflict monitoring and decision making: reconciling two perspectives on anterior cingulate function. Cognit. Affect Behav. Neurosci. 7 (4), 356–366.
Boy, F., Evans, C.J., Edden, R.A., Singh, K.D., Husain, M., Sumner, P., 2010. Individual differences in subconscious motor control predicted by GABA concentration in SMA. Curr. Biol. 20 (19), 1779–1785. https://doi.org/10.1016/j.cub.2010.09.003.
Brainard, D.H., Vision, S., 1997. The psychophysics toolbox. Spatial Vis. 10, 433–436.
Braver, T.S., Krug, M.K., Chiew, K.S., Kool, W., Westbrook, J.A., Clement, N.J., Carver, C.S., 2014. Mechanisms of motivation–cognition interaction: challenges and opportunities. Cognit. Affect Behav. Neurosci. 14 (2), 443–472.
Cerasoli, C.P., Nicklin, J.M., Ford, M.T., 2014. Intrinsic motivation and extrinsic incentives jointly predict performance: a 40-year meta-analysis. Psychol. Bull. 140 (4), 980.
Croxson, P.L., Walton, M.E., O'Reilly, J.X., Behrens, T.E., Rushworth, M.F., 2009. Effort-based cost–benefit valuation and the human brain. J. Neurosci. 29 (14), 4531–4541.
Dayan, P., Niv, Y., 2008. Reinforcement learning: the good, the bad and the ugly. Curr. Opin. Neurobiol. 18 (2), 185–196.
De Graaf, R.A., 2013. In Vivo NMR Spectroscopy: Principles and Techniques. John Wiley & Sons.
Donahue, M.J., Near, J., Blicher, J.U., Jezzard, P., 2010. Baseline GABA concentration and fMRI response. Neuroimage 53 (2), 392–398.
Etzel, J.A., Cole, M.W., Zacks, J.M., Kay, K.N., Braver, T.S., 2015. Reward motivation enhances task coding in frontoparietal cortex. Cerebr. Cortex 26 (4), 1647–1659.
Floyer-Lea, A., Wylezinska, M., Kincses, T., Matthews, P.M., 2006. Rapid modulation of GABA concentration in human sensorimotor cortex during motor learning. J. Neurophysiol. 95 (3), 1639–1644.
Gasparovic, C., Song, T., Devier, D., Bockholt, H.J., Caprihan, A., Mullins, P.G., Morrison, L.A., 2006. Use of tissue water as a concentration reference for proton spectroscopic imaging. Magn. Reson. Med. 55 (6), 1219–1226. https://doi.org/10.1002/mrm.20901.
Gussew, A., Rzanny, R., Erdtel, M., Scholle, H.C., Kaiser, W.A., Mentzel, H.J., Reichenbach, J.R., 2010. Time-resolved functional 1H MR spectroscopic detection of glutamate concentration changes in the brain during acute heat pain stimulation. Neuroimage 49 (2), 1895–1902. https://doi.org/10.1016/j.neuroimage.2009.09.007.
Haber, S.N., Knutson, B., 2010. The reward circuit: linking primate anatomy and human imaging. Neuropsychopharmacology 35 (1), 4.
Hasler, G., van der Veen, J.W., Grillon, C., Drevets, W.C., Shen, J., 2010. Effect of acute psychological stress on prefrontal GABA concentration determined by proton magnetic resonance spectroscopy. Am. J. Psychiatr. 167 (10), 1226–1231.
Heilbronner, S.R., Hayden, B.Y., 2016. Dorsal anterior cingulate cortex: a bottom-up view. Annu. Rev. Neurosci. 39 (39), 149–170. https://doi.org/10.1146/annurev-neuro-070815-013952.
Hosking, J.G., Cocker, P.J., Winstanley, C.A., 2014. Dissociable contributions of anterior cingulate cortex and basolateral amygdala on a rodent cost/benefit decision-making task of cognitive effort. Neuropsychopharmacology 39 (7), 1558.
Isaacson, J.S., Scanziani, M., 2011. How inhibition shapes cortical activity. Neuron 72 (2), 231–243.
Jocham, G., Hunt, L.T., Near, J., Behrens, T.E., 2012. A mechanism for value-guided choice based on the excitation-inhibition balance in prefrontal cortex. Nat. Neurosci. 15 (7), 960–961.
Johansen, J.P., Cain, C.K., Ostroff, L.E., LeDoux, J.E., 2011. Molecular mechanisms of fear learning and memory. Cell 147 (3), 509–524.
Kegeles, L.S., Mao, X., Gonsalez, R., Shungu, D.C., 2007. Evaluation of anatomic variation in macromolecule contribution to the GABA signal using metabolite nulling and the J-editing technique at 3T. In: Paper Presented at the Proceedings of the 15th Annual Meeting of ISMRM, Berlin, Germany.
Kelley, A.E., 2004. Ventral striatal control of appetitive motivation: role in ingestive behavior and reward-related learning. Neurosci. Biobehav. Rev. 27 (8), 765–776.
Kennerley, S.W., Walton, M.E., Behrens, T.E., Buckley, M.J., Rushworth, M.F., 2006. Optimal decision making and the anterior cingulate cortex. Nat. Neurosci. 9 (7), 940.
Kolling, N., Wittmann, M.K., Behrens, T.E., Boorman, E.D., Mars, R.B., Rushworth, M.F., 2016. Value, search, persistence and model updating in anterior cingulate cortex. Nat. Neurosci. 19 (10), 1280–1285.
Kuhn, S., Schubert, F., Mekle, R., Wenger, E., Ittermann, B., Lindenberger, U., Gallinat, J., 2016. Neurotransmitter changes during interference task in anterior cingulate cortex: evidence from fMRI-guided functional MRS at 3 T. Brain Struct. Funct. 221 (5), 2541–2551. https://doi.org/10.1007/s00429-015-1057-0.
Lally, N., Mullins, P.G., Roberts, M.V., Price, D., Gruber, T., Haenschel, C., 2014. Glutamatergic correlates of gamma-band oscillatory activity during cognition: a concurrent ER-MRS and EEG study. Neuroimage 85 (Pt 2), 823–833. https://doi.org/10.1016/j.neuroimage.2013.07.049.
Lee, D., Seo, H., Jung, M.W., 2012. Neural basis of reinforcement learning and decision making. Annu. Rev. Neurosci. 39 (35), 287–308. https://doi.org/10.1146/annurev-neuro-062111-150512.
Letzkus, J.J., Wolff, S.B., Meyer, E.M., Tovote, P., Courtin, J., Herry, C., Lüthi, A., 2011. A disinhibitory microcircuit for associative fear learning in the auditory cortex. Nature 480 (7377), 331.
Levar, N., van Leeuwen, J.M., Puts, N.A., Denys, D., van Wingen, G.A., 2017. GABA concentrations in the anterior cingulate cortex are associated with fear network function and fear recovery in humans. Front. Hum. Neurosci. 11.
Mangia, S., Giove, F., Bianciardi, M., Di Salle, F., Garreffa, G., Maraviglia, B., 2003. Issues concerning the construction of a metabolic model for neuronal activation. J. Neurosci. Res. 71 (4), 463–467. https://doi.org/10.1002/jnr.10531.
Mangia, S., Giove, F., Tkac, I., Logothetis, N.K., Henry, P.G., Olman, C.A., Ugurbil, K., 2009. Metabolic and hemodynamic events after changes in neuronal activity: current hypotheses, theoretical predictions and in vivo NMR experimental findings. J. Cerebr. Blood Flow Metabol. 29 (3), 441–463. https://doi.org/10.1038/jcbfm.2008.134.
Mangia, S., Tkáč, I., Gruetter, R., Van de Moortele, P.-F., Maraviglia, B., Uğurbil, K., 2007a. Sustained neuronal activation raises oxidative metabolism to a new steady-state level: evidence from 1H NMR spectroscopy in the human visual cortex. J. Cerebr. Blood Flow Metabol. 27 (5), 1055–1063.
Mangia, S., Tkac, I., Gruetter, R., Van de Moortele, P.F., Maraviglia, B., Ugurbil, K., 2007b. Sustained neuronal activation raises oxidative metabolism to a new steady-state level: evidence from 1H NMR spectroscopy in the human visual cortex. J. Cerebr. Blood Flow Metabol. 27 (5), 1055–1063. https://doi.org/10.1038/sj.jcbfm.9600401.
Medalla, M., Barbas, H., 2009. Synapses with inhibitory neurons differentiate anterior cingulate from dorsolateral prefrontal pathways associated with cognitive control. Neuron 61 (4), 609–620.
Mescher, M., Merkle, H., Kirsch, J., Garwood, M., Gruetter, R., 1998. Simultaneous in vivo spectral editing and water suppression. NMR Biomed. 11, 266–272. EPFL-ARTICLE-177509.
Michels, L., Martin, E., Klaver, P., Edden, R., Zelaya, F., Lythgoe, D.J., O'Gorman, R.L., 2012. Frontal GABA levels change during working memory. PLoS One 7 (4), e31933. https://doi.org/10.1371/journal.pone.0031933.

Mullins, P.G., 2018. Towards a theory of functional magnetic resonance spectroscopy (fMRS): a meta-analysis and discussion of using MRS to measure changes in neurotransmitters in real time. Scand. J. Psychol. 59 (1), 91–103. https://doi.org/10.1111/sjop.12411.

Mullins, P.G., McGonigle, D.J., O'gorman, R.L., Puts, N.A., Vidyasagar, R., Evans, C.J., Edden, R.A., 2014. Current practice in the use of MEGA-PRESS spectroscopy for the detection of GABA. Neuroimage 86, 43–52.

Murphy, B.K., Miller, K.D., 2009. Balanced amplification: a new mechanism of selective amplification of neural activity patterns. Neuron 61 (4), 635–648.

Muthukumaraswamy, S.D., Edden, R.A., Jones, D.K., Swettenham, J.B., Singh, K.D., 2009. Resting GABA concentration predicts peak gamma frequency and fMRI amplitude in response to visual stimulation in humans. Proc. Natl. Acad. Sci. Unit. States Am. 106 (20), 8356–8361.

Myhrer, T., 2003. Neurotransmitter systems involved in learning and memory in the rat: a meta-analysis based on studies of four behavioral tasks. Brain Res. Rev. 41 (2), 268–287.

Northoff, G., Walter, M., Schulte, R.F., Beck, J., Dydak, U., Henning, A., Boesiger, P., 2007. GABA concentrations in the human anterior cingulate cortex predict negative BOLD responses in fMRI. Nat. Neurosci. 10 (12), 1515.

Payzan-LeNestour, E., Dunne, S., Bossaerts, P., O'Doherty, J.P., 2013. The neural representation of unexpected uncertainty during value-based decision making. Neuron 79 (1), 191–201.

Prévost, C., Pessiglione, M., Météreau, E., Cléry-Melin, M.-L., Dreher, J.-C., 2010. Separate valuation subsystems for delay and effort decision costs. J. Neurosci. 30 (42), 14080–14090.

Ramadan, S., Lin, A., Stanwell, P., 2013. Glutamate and glutamine: a review of in vivo MRS in the human brain. NMR Biomed. 26 (12), 1630–1646. https://doi.org/10.1002/nbm.3045.

Ridderinkhof, K.R., Ullsperger, M., Crone, E.A., Nieuwenhuis, S., 2004. The role of the medial frontal cortex in cognitive control. Science 306 (5695), 443–447.

Rudebeck, P.H., Walton, M.E., Smyth, A.N., Bannerman, D.M., Rushworth, M.F., 2006. Separate neural pathways process different decision costs. Nat. Neurosci. 9 (9), 1161.

Sampaio-Baptista, C., Filippini, N., Stagg, C.J., Near, J., Scholz, J., Johansen-Berg, H., 2015. Changes in functional connectivity and GABA levels with long-term motor learning. Neuroimage 106, 15–20. https://doi.org/10.1016/j.neuroimage.2014.11.032.

Sanaei Nezhad, F., Anton, A., Michou, E., Jung, J., Parkes, L.M., Williams, S.R., 2018. Quantification of GABA, glutamate and glutamine in a single measurement at 3 T using GABA-edited MEGA-PRESS. NMR Biomed. 31 (1) https://doi.org/10.1002/nbm.3847.

Schmitz, T.W., Correia, M.M., Ferreira, C.S., Prescot, A.P., Anderson, M.C., 2017. Hippocampal GABA enables inhibitory control over unwanted thoughts. Nat. Commun. 8 (1), 1311. https://doi.org/10.1038/s41467-017-00956-z.

Shenhav, A., Botvinick, M.M., Cohen, J.D., 2013. The expected value of control: an integrative theory of anterior cingulate cortex function. Neuron 79 (2), 217–240.

Shenhav, A., Cohen, J.D., Botvinick, M.M., 2016. Dorsal anterior cingulate cortex and the value of control. Nat. Neurosci. 19 (10), 1286–1291.

Sheth, S.A., Mian, M.K., Patel, S.R., Asaad, W.F., Williams, Z.M., Dougherty, D.D., Eskandar, E.N., 2012. Human dorsal anterior cingulate cortex neurons mediate ongoing behavioral adaptation. Nature 488 (7410), 218.

Stagg, C.J., Bachtiar, V., Johansen-Berg, H., 2011. What are we measuring with GABA magnetic resonance spectroscopy? Commun. Integr. Biol. 4 (5), 573–575. https://doi.org/10.4161/cib.4.5.16213.

Stanley, J.A., Burgess, A., Khatib, D., Ramaseshan, K., Arshad, M., Wu, H., Diwadkar, V.A., 2017. Functional dynamics of hippocampal glutamate during associative learning assessed with in vivo (1)H functional magnetic resonance spectroscopy. Neuroimage 153, 189–197. https://doi.org/10.1016/j.neuroimage.2017.03.051.

Sumner, P., Edden, R.A., Bompas, A., Evans, C.J., Singh, K.D., 2010. More GABA, less distraction: a neurochemical predictor of motor decision speed. Nat. Neurosci. 13 (7), 825–827. https://doi.org/10.1038/nn.2559.

Taylor, R., Schaefer, B., Densmore, M., Neufeld, R.W., Rajakumar, N., Williamson, P.C., Theberge, J., 2015. Increased glutamate levels observed upon functional activation in the anterior cingulate cortex using the Stroop Task and functional spectroscopy. Neuroreport 26 (3), 107–112. https://doi.org/10.1097/WNR.0000000000000309.

Treviño, M., 2016. Inhibition controls asynchronous states of neuronal networks. Front. Synaptic Neurosci. 8.

Van Vreeswijk, C., Sompolinsky, H., 1996. Chaos in neuronal networks with balanced excitatory and inhibitory activity. Science 274 (5293), 1724–1726.

Vogels, T.P., Sprekeler, H., Zenke, F., Clopath, C., Gerstner, W., 2011. Inhibitory plasticity balances excitation and inhibition in sensory pathways and memory networks. Science 334 (6062), 1569–1573.

Wagenmakers, E.J., Marsman, M., Jamil, T., Ly, A., Verhagen, J., Love, J., Morey, R.D., 2018. Bayesian inference for psychology. Part I: theoretical advantages and practical ramifications. Psychon. Bull. Rev. 25 (1), 35–57. https://doi.org/10.3758/s13423-017-1343-3.

Walton, M.E., Croxson, P.L., Behrens, T.E., Kennerley, S.W., Rushworth, M.F., 2007. Adaptive decision making and value in the anterior cingulate cortex. Neuroimage 36, T142–T154.

Yizhar, O., Fenno, L.E., Prigge, M., Schneider, F., Davidson, T.J., O'Shea, D.J., Paz, J.T., 2011. Neocortical excitation/inhibition balance in information processing and social dysfunction. Nature 477 (7363), 171–178.

Yoon, J.H., Grandelis, A., Maddock, R.J., 2016. Dorsolateral prefrontal cortex GABA concentration in humans predicts working memory load processing capacity. J. Neurosci. 36 (46), 11788–11794.